

Complex liquid crystal alignments accomplished by Talbot self-imaging

Xi-kui Hu,¹ Bing-yan Wei,¹ Xiao-wen Lin,¹ Wei Hu,^{1,3} Ge Zhu,¹ Vladimir Chigrinov,²
and Yan-qing Lu^{1,*}

¹ National Laboratory of Solid State Microstructures and College of Engineering and Applied Sciences, Nanjing University, Nanjing 210093, China

² Center for Display Research, Department of Electronic and Computer Engineering, Hong Kong University of Science and Technology, Clear Water Bay, Kowloon, Hong Kong, China

³ huwei@nju.edu.cn

* yqlu@nju.edu.cn

Abstract: We introduce Talbot self-imaging into photoalignment technique to record Talbot carpet into an LC cell. Through the design of the setup, different images are presented on a single sample. By taking a simple 1D grating mask as an example, an LC cell with complex alignment structures applicable as Mach-Zehnder interferometer arrays is demonstrated. Further mask design permits feasibility of various structures which are practicable for many applications. This method may facilitate the fabrication of photonic applications such as optical communication, computing and sensing, etc.

©2013 Optical Society of America

OCIS codes: (160.3710) Liquid crystals; (070.6760) Talbot and self-imaging effects; (080.1238) Array waveguide devices.

References and links

1. Y. H. Lin, H. W. Ren, Y. H. Wu, Y. Zhao, J. Y. Fang, Z. B. Ge, and S. T. Wu, "Polarization-independent liquid crystal phase modulator using a thin polymer-separated double-layered structure," *Opt. Express* **13**(22), 8746–8752 (2005).
2. Y. H. Wu, Y. H. Lin, Y. Q. Lu, H. Ren, Y. H. Fan, J. Wu, and S. T. Wu, "Submillisecond response variable optical attenuator based on sheared polymer network liquid crystal," *Opt. Express* **12**(25), 6382–6389 (2004).
3. H. W. Ren, D. Fox, P. A. Anderson, B. Wu, and S. T. Wu, "Tunable-focus liquid lens controlled using a servo motor," *Opt. Express* **14**(18), 8031–8036 (2006).
4. J. Feng, Y. Zhao, S. S. Li, X. W. Lin, F. Xu, and Y. Q. Lu, "Fiber optic pressure sensor based on tunable liquid crystal technology," *IEEE Photon. J.* **2**(3), 292–298 (2010).
5. X. W. Lin, J. B. Wu, W. Hu, Z. G. Zheng, Z. J. Wu, G. Zhu, F. Xu, B. B. Jin, and Y. Q. Lu, "Self-polarizing terahertz liquid crystal phase shifter," *AIP Adv.* **1**(3), 032133 (2011).
6. D. K. Yang and S. T. Wu, eds., *Fundamentals of Liquid Crystal Devices* (Wiley, 2006).
7. V. G. Chigrinov, V. M. Kozenkov, and H. S. Kwok, eds., *Photoalignment of Liquid Crystalline Materials: Physics and Applications* (Wiley, 2008).
8. O. Yaroshchuk and Y. Reznikov, "Photoalignment of liquid crystals: basics and current trends," *J. Mater. Chem.* **22**(2), 286–300 (2011).
9. V. Kapoustine, A. Kazakevitch, V. So, and R. Tam, "Simple method of formation of switchable liquid crystal gratings by introducing periodic photoalignment pattern into liquid crystal cell," *Opt. Commun.* **266**(1), 1–5 (2006).
10. X. Zhao, A. Bermak, F. Boussaid, T. Du, and V. G. Chigrinov, "High-resolution photoaligned liquid-crystal micropolarizer array for polarization imaging in visible spectrum," *Opt. Lett.* **34**(23), 3619–3621 (2009).
11. H. Akiyama, T. Kawara, H. Takada, H. Takatsu, V. Chigrinov, E. Prudnikova, V. Kozenkov, and H. Kwok, "Synthesis and properties of azo dye aligning layers for liquid crystal cells," *Liq. Cryst.* **29**(10), 1321–1327 (2002).
12. M. Schadt, H. Seiberle, and A. Schuster, "Optical patterning of multi-domain liquid-crystal displays with wide viewing-angles," *Nature* **381**(6579), 212–215 (1996).
13. S. Y. Huang, S. T. Wu, and A. Y. G. Fuh, "Optically switchable twist nematic grating based on a dye-doped liquid crystal film," *Appl. Phys. Lett.* **88**(4), 041104 (2006).
14. W. Y. Wu and A. Y. G. Fuh, "Rewritable liquid crystal gratings fabricated using photoalignment effect in dye-doped poly(vinyl alcohol) film," *Jpn. J. Appl. Phys.* **46**(10A), 6761–6766 (2007).
15. V. Presnyakov, K. Asatryan, T. Galstian, and V. Chigrinov, "Optical polarization grating induced liquid crystal micro-structure using azo-dye command layer," *Opt. Express* **14**(22), 10558–10564 (2006).

16. W. Hu, A. Srivastava, F. Xu, J. T. Sun, X. W. Lin, H. Q. Cui, V. Chigrinov, and Y. Q. Lu, "Liquid crystal gratings based on alternate TN and PA photoalignment," *Opt. Express* **20**(5), 5384–5391 (2012).
17. W. Hu, A. Kumar Srivastava, X.-W. Lin, X. Liang, Z.-J. Wu, J.-T. Sun, G. Zhu, V. Chigrinov, and Y.-Q. Lu, "Polarization independent liquid crystal gratings based on orthogonal photoalignments," *Appl. Phys. Lett.* **100**(11), 111116 (2012).
18. X. W. Lin, W. Hu, X. K. Hu, X. Liang, Y. Chen, H. Q. Cui, G. Zhu, J. N. Li, V. Chigrinov, and Y. Q. Lu, "Fast response dual-frequency liquid crystal switch with photo-patterned alignments," *Opt. Lett.* **37**(17), 3627–3629 (2012).
19. H. F. Talbot, "Facts relating to optical science, No. IV," *Philos. Mag.* **9**, 401–407 (1836).
20. K. Patorski, "The self-imaging phenomenon and its applications," *Prog. Opt.* **27**, 1–108 (1989).
21. A. Isoyan, F. Jiang, Y. C. Cheng, F. Cerrina, P. Wachulak, L. Urbanski, J. Rocca, C. Menoni, and M. Marconi, "Talbot lithography: Self-imaging of complex structures," *J. Vac. Sci. Technol. B* **27**(6), 2931–2937 (2009).
22. L. Stuerzebecher, T. Harzendorf, U. Vogler, U. D. Zeitner, and R. Voelkel, "Advanced mask aligner lithography: Fabrication of periodic patterns using pinhole array mask and Talbot effect," *Opt. Express* **18**(19), 19485–19494 (2010).
23. L. B. Soldano and E. C. M. Pennings, "Optical multi-mode interference devices based on self-imaging: principles and applications," *J. Lightwave Technol.* **13**(4), 615–627 (1995).
24. S. R. Nersisyan, N. V. Tabiryan, D. M. Steeves, B. R. Kimball, V. G. Chigrinov, and H. S. Kwok, "Study of azo dye surface command photoalignment material for photonics applications," *Appl. Opt.* **49**(10), 1720–1727 (2010).
25. I. Abdulhalim, "Liquid crystal active nanophotonics and plasmonics: from science to devices," *J. Nanophotonics* **6**(1), 061001 (2012).
26. A. Peruzzo, A. Laing, A. Politi, T. Rudolph, and J. L. O'Brien, "Multimode quantum interference of photons in multiport integrated devices," *Nat Commun* **2**, 224 (2011).
27. P. J. Shadbolt, M. R. Verde, A. Peruzzo, A. Politi, A. Laing, M. Lobino, J. C. F. Matthews, M. G. Thompson, and J. L. O'Brien, "Generating, manipulating and measuring entanglement and mixture with a reconfigurable photonic circuit," *Nat. Photonics* **6**(1), 45–49 (2011).
28. B. J. Metcalf, N. Thomas-Peter, J. B. Spring, D. Kundys, M. A. Broome, P. C. Humphreys, X.-M. Jin, M. Barbieri, W. Steven Kolthammer, J. C. Gates, B. J. Smith, N. K. Langford, P. G. R. Smith, and I. A. Walmsley, "Multiphoton quantum interference in a multiport integrated photonic device," *Nat Commun* **4**, 1356 (2013).

1. Introduction

Liquid crystal (LC) components have been widely used in flat panel display, optical communication and sensing [1–6] for their advantages of low power consumption, compact size, no moving parts and reliable performance. High quality LC alignment is crucial for good performance of most LC devices that consist of rod-like nematic LC molecules. Among various alignment techniques, photoalignment is considered as a promising one [7, 8]. It can accomplish high quality LC alignment with resolution up to 1 μm [9, 10], and totally avoids the problems resulting from the conventional rubbing method, such as contamination, electrostatic charges and mechanical damage [11]. In addition, it also simplifies the fabrication of multi-domain LC alignments, which are beneficial to the wide viewing angles in liquid crystal displays [12] and various photonic applications [9, 13, 14]. Both laser interference [15] and UV exposure with amplitude masks [9] have been proposed, which are suitable for simple patterns such as 1D and 2D gratings [14, 16–18]. However, for more complex structures, specially designed photo mask is necessary, causing increase in cost and decrease in efficiency. Therefore new approaches towards generating complex LC alignments with high efficiency are much desired.

In exploring such approaches, Talbot effect, a basically near-field diffraction phenomenon [19, 20], has attracted our attention. When a monochromatic coherent light illuminates on a periodic structure, images periodically replicate at certain distances. By means of such self-imaging approach, complex patterns could be generated just utilizing a simple periodic photo mask [21–23]. Besides convenience in fabrication, high resolution up to optical limit is also one of its major advantages. Therefore, it is worth trying to introduce Talbot effect into photoalignment technology.

In this work, we design an exposing setup to form structured LC alignments through Talbot self-imaging. Herein, as an example, we choose a simple 1D grating as the photo mask. The setup parameters are selected through simulation and then the expected patterns in LC alignments are realized, which are coincident with simulation results. Moreover, the applicability of this approach into future applications like Mach-Zehnder interferometers

(MZIs) are further discussed. More complex structures could also be achieved through mask design, bringing potential applications in integrated optics.

2. Design and experiment

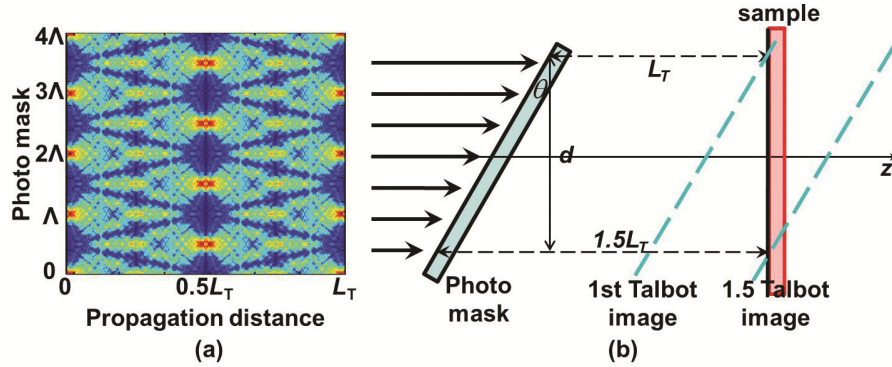


Fig. 1. (a) Simulated Talbot carpet and (b) Schematic illustration of Talbot self-imaging based photoalignment.

Talbot effect is a near-field self-imaging phenomenon. When a plane wave illuminates onto a photo mask, e.g. a 1D grating, images will periodically change with different distances resulting from the light diffraction. As shown in Fig. 1(a), at the eigen Talbot distance L_T , where the phase difference between the different diffracted light is integer multiples of 2π , the pattern is exactly the same as that of photo mask. At $0.5 L_T$, image is still same with the photo mask but has a lateral displacement of half grating period ($\Lambda/2$). Between photo mask and L_T , images change continuously and form a Talbot carpet. Here L_T has a simple relationship with Λ and incident light wavelength λ ,

$$L_T = 2\Lambda^2/\lambda. \quad (1)$$

In our design (Fig. 1(b)) the photo mask is tilted with an angle θ , and the Talbot images would follow the tilt. Then on a vertically placed sample, different patterns would occur within a vertical distance d . As an example, we record the images between L_T and $1.5 L_T$ on the sample. The relationship between d and L_T can be described as,

$$\tan \theta = \frac{1.5L_T - L_T}{d}. \quad (2)$$

Due to the tilt of photo mask, the actual pattern period on the sample (L'_T) is different from L_T . Herein $d = L_T/2$, then the relationship between L'_T and L_T is,

$$L'_T = L_T \cot \theta. \quad (3)$$

That is to say, Talbot carpet can be compressed or stretched by tilting the mask with different angles.

In our experiment, the light source is a solid state laser (405 nm, 60 mW/cm²). The expanded beam ($\Phi = 2$ cm, which is the diameter of the extended beam) goes through a polarizer and illuminates onto the titled mask with $\theta = 45^\circ$. The mask is a 1D grating with period $\Lambda = 50$ μm and duty cycle $\eta = 1:3$. According to Eq. (1), $L_T = 1.23$ cm. The simulated Talbot carpet is shown in Fig. 2(a).

The sample is an ITO glass substrate spin-coated with SD1 layer, the molecules of which tend to orient perpendicularly to the light polarization [24]. Two pieces of such samples are pre-aligned by a uniform linearly polarized blue light at a dose of 5 J/cm². Then one of them is set in the Talbot self-imaging setup (Fig. 1(b)) and exposed again with the same dose while

the incident polarization is perpendicular to that of the pre-exposure. SD1 shows excellent alignment rewritability [7], therefore a replica pattern of Talbot carpet is recorded with a perpendicular orientation compared to surrounding areas.

The two samples are then assembled to make an LC cell, separated by 4 μm spacers. Then we infiltrate LC mixture E7 ($n_e = 1.7429$ and $n_o = 1.5198$) into the cell at isotropic state. After cooling down to room temperature, the LC molecules are guided by SD1 and form twisted nematic (TN) in Talbot carpet region and homogeneous alignment (PA) in surrounding areas respectively. Herein TN/PA bi-domain alignment is demonstrated to facilitate the observation. Orthogonal PA image is also achievable [17], which could supply the largest contrast in refractive index between the two domains. Herein, the duty cycle of our grating mask is 1:3; however, according to the principle of Talbot self-imaging, grating mask with any duty cycle could work. Figure 2(b) exhibits an image of the cell under a polarizing microscope with crossed polarizers. The bright pattern is quite coincident with the simulated Talbot carpet (Fig. 2(a)). However, some fine structures are not clearly exhibited in the experimental result. The main reason is attributed to the quality of the light source we used. The intensity of the light source is not very uniform and its coherence is not very good, which limit the experimental quality of self-imaging.

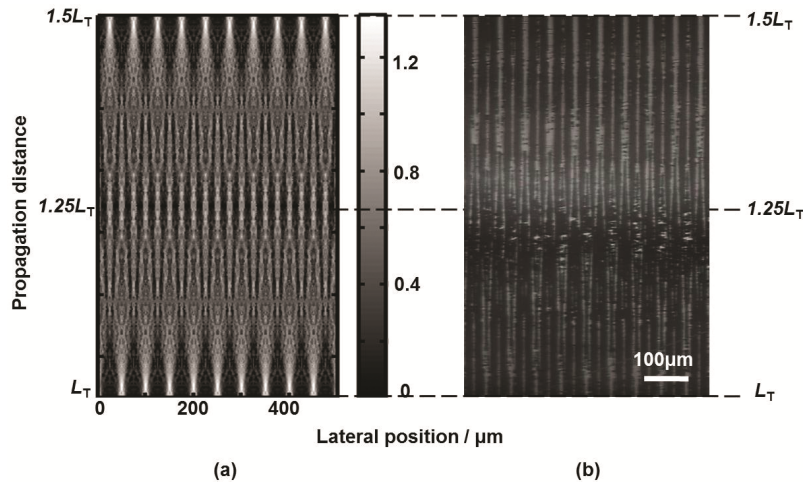


Fig. 2. (a) Theoretical and (b) experimental Talbot carpets of 1D grating, taken under a polarizing microscope with crossed polarizers.

3. Discussions and prospects

As revealed in Fig. 2(b), one single bright strip gradually splits into two and then the separated two strips merge back into one. This whole pattern is quite similar to a Mach-Zehnder interferometer (MZI) array. As we know, LC normally has a quite large birefringence, thus different alignment domains should have a remarkable refractive index contrast for a specified polarization state. As long as a light beam is coupled into the LC layer, light would more concentrate in the high index waveguide channels then propagate forward. Interference may happen if two channels combine together. Due to the tunability nature of LC, this kind of “MZI” is even tunable. To implement such a design, patterned electrodes on the two substrates are needed in order to apply voltages to one arm (one of the splitted channels) while keeping the other arm out of the electric field. The LC pre-alignment in both two arms should be parallel to incident light polarization, so the initial refractive indices in the arms are n_e . On the contrary, the initial refractive index in the background region (the regions around the strips) are set to be n_o . The above design is illustrated in Fig. 3(a). When an electric field is applied to one arm, the effective refractive index n_{eff} of the LCs

in this arm gradually turns from n_e to n_o , while that of the other arm is kept as n_e and that of the background region remains n_o . Thus a tunable MZI is realized.

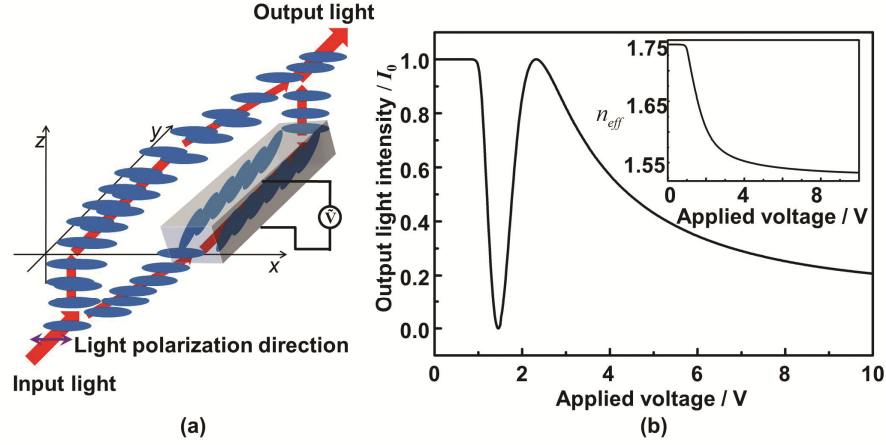


Fig. 3. (a) Schematic of an LC MZI and (b) theoretical V - T curve of the output light, inset is V - n_{eff} curve.

Taking a 4- μm -thick E7 cell as an example, we assume the length of one separate arm $l = 10 \mu\text{m}$, and thus the phase difference between the two arms is,

$$\Delta\phi = \frac{2\pi(n_e - n_{\text{eff}})l}{\lambda}. \quad (4)$$

Here, λ is the signal wavelength fixed at $1.55 \mu\text{m}$. With no loss of generality, assume the two MZI arms split the light equally, and thus the corresponding output light intensity is,

$$T(V) = I_0 \cos^2 \Delta\phi. \quad (5)$$

The voltage dependent output intensity (V - T) curve is calculated as shown in Fig. 3(b), and the inset is the V - n_{eff} curve. The intensity can be tuned continuously between 0 and I_0 by applying different voltages.

We prove through the above experiments and discussions the applicability of generating complex alignment structures by a simple mask through the LC alignment technique based on Talbot self-imaging. Further mask design permits feasibility of more complex combinations of Y-junctions and MZIs, which have great potentials in micro/nano photonics [25], integrated optics [26], and even quantum optics [27]. For example, multiport waveguide circuits have been employed in quantum information technologies such as quantum walk and multi-photon interference [26–28]. Our approach could supply a simple way for the preparation of high resolution and large area waveguide networks. We believe the introduction of Talbot self-imaging based photoalignment may facilitate the fabrication of photonic applications such as optical communication, computing and sensing, etc.

4. Conclusion

In summary, we introduce Talbot self-imaging into LC photoalignment and utilize a simple 1D grating as the photo mask to generate patterned LC alignments. Through this simple and efficient approach, high resolution and large area structures could be obtained. Waveguide arrays constructed by Y-junctions and Mach-Zehnder interferometers are prospected and discussed. More complex structures could also be achieved through mask design, bringing potential applications in integrated optics and quantum photonics.

Acknowledgments

The authors thank Yang Ming for his constructive discussions. This work is sponsored by 973 programs with contract No. 2011CBA00200 and 2012CB921803, National Science Fund for Distinguished Young Scholars with contract No. 61225026, HKUST grant CERG 612310, Research Fund for the Doctoral Program of Higher Education of China with contract No. 20120091120020. Correspondences about this paper should be addressed to Dr. Wei Hu or Prof. Yan-qing Lu.